J Math Chem (2013) 51:588–602
DOI 10.1007/s10910-012-0099-2

ORIGINAL PAPER

Entropy production of a mechanically driven single oligomeric enzyme: a consequence of fluctuation theorem

Biswajit Das · Kinshuk Banerjee · Gautam Gangopadhyay

Received: 18 August 2012 / Accepted: 24 September 2012 / Published online: 16 October 2012

Abstract In this work we have shown how an applied mechanical force affects an oligomeric enzyme kinetics in a chemiostatic condition where the statistical characteristics of random walk of the substrate molecules over a finite number of active sites of the enzyme plays important contributing factors in governing the overall rate and nonequilibrium thermodynamic properties. The analytical results are supported by the simulation of single trajectory based approach of entropy production using Gillespie's stochastic algorithm. This microscopic numerical approach not only gives the macroscopic entropy production from the mean of the distribution of entropy production which depends on the force but also a broadening of the distribution by the applied mechanical force, a kind of power broadening. In the nonequilibrium steady state (NESS), both the mean and the variance of the distribution increases and then saturates with the rise in applied force corresponding to the situation when the net rate of product formation reaches a limiting value with an activationless transition. The effect of the system-size and force on the entropy production distribution is shown to be constrained by the detailed fluctuation theorem.

Keywords Oligomeric enzyme kinetics · Nonequilibrium steady state · Single trajectory analysis · Fluctuation theorem

1 Introduction

In the last few years, stochastic non-equilibrium dynamics have become a major research area to describe the thermodynamics of the mechanochemical processes at

B. Das · K. Banerjee · G. Gangopadhyay (✉)
S. N. Bose National Centre for Basic Sciences, Block-JD, Sec-III, Salt Lake, Kolkata 700098, India
e-mail: gautam@bose.res.in

the single molecule level [1–11]. One can attach a molecule to the tip of a cantilever of an atomic force microscope to apply the external mechanical force on a single molecule which can drive the whole system far away from equilibrium. Very often this force can change the thermodynamic stability of a molecule and can modify the reaction rates [12,13]. To describe the effect of force and to give the thermodynamic description of such non-equilibrium single molecule processes, trajectory analysis is the standard tool already developed in stochastic non-equilibrium thermodynamics [8,10,11]. Trajectory analysis gives fundamental relations known as the fluctuation theorems describing the statistical fluctuations in time-averaged properties of many-particle systems in far away from equilibrium states [14–25]. Using these relations one can understand how macroscopic irreversibility emerges from microscopically reversible dynamics [16,26]. Stochastic trajectory approach has been successfully applied to various systems, e.g, chemical reaction networks [27], driven colloidal particles [28], single two level systems [29] and also single bio-molecular reactions [30,31].

Although mechanical stress is known to profoundly influence the composition and structure of the proteins and enzyme, the mechanism of the force induced chemical processes [32–35] can ideally be probed through the single molecule reaction [36–38]. Recently Fernandez et al. [32,33] and Gumpp et al. [34] have opened a new avenue to study the direct influence of external mechanical force to manipulate the biocatalytic reaction of an enzyme by triggering the enzymatic activity through atomic force microscopy (AFM). In this context, we have theoretically studied the effect of external mechanical force on a single oligomeric enzyme kinetics at a chemiostatic condition with the substrate and product concentrations remaining constant [39].It was found that the net rate of the reaction averaged over several turn over cycles in chemiostatic condition was multiplied by the number of active sites and got further enhanced by more than two orders of magnitude with the application of 10–100 pN force [39].

Here we have studied the nonequilibrium thermodynamic properties of an external force induced oligomeric enzyme catalysis. The statistical characteristics of binding of substrate molecules over a finite number of active sites on a single enzyme is formulated through a master equation which is used to calculate the entropy production. We have also numerically obtained the microscopic picture of the entropy production through the single stochastic trajectory analysis [18,27,28,40] using the Gillespie's stochastic simulation approach. Although in the recent literature a great deal of effort has been utilized on the exploration of the validity of the fluctuation theorem in various mechanical and chemical systems, the attempt to find out the nonequilibrium dynamical properties as a consequence of the fluctuation theorem is not yet explored with its full potential. Here it is shown how the trajectory based approach can provide the effect of mechanical force in terms of the distribution of the entropy production that can not be obtained from the analytical method of calculation of entropy production specially for the small system.

The paper is organized as follows. In Sect. 2, we have provided the scheme of the reaction and the master equation suitable for the calculation of the various entropy production rates. The simulation procedure for the single trajectory entropy calculation is described in Sect. 3. The numerical results of the various entropy productions of the reaction system as a function of the force parameter are discussed in Sect. 4. The paper is concluded in Sect. 5.

2 Description of single oligomeric enzyme kinetics and entropy production

In this section, first we have provided the master equation describing the single oligomeric enzyme kinetics suitable for the calculation of entropy production. Then from the traditional approach the corresponding expressions of the system, medium and total entropy production rates are given from the overall dynamics of the reaction.

2.1 Scheme of the reaction and the master equation

Single molecule enzyme kinetics are usually studied at the chemiostatic condition where the concentrations of substrate, S and product, P are maintained at constant values. In chemiostatic condition, the traditional bulk enzyme kinetics reaction scheme (see Fig. 1a) can be reformulated in a simplified manner which is shown in Fig. 1b. In our case, the oligomeric enzyme consists of n_T number of identical subunits and each sub-unit has one active site. The subunits are linked through extra covalent bonding by using some cross linking reagents [41]. As each active site can form one ES-complex, so the reaction scheme can be viewed in terms of the number of total active sites present at a particular time in the oligomeric enzyme. Here, the active sites which have already formed ES-complex are referred to as occupied sites and those lying vacant at that moment are called the vacant sites.The scheme of the oligomeric enzyme catalyzed reaction in bulk and in chemiostatic condition are depicted in Fig. 1c, d. The rate constants $K_1 = (k_1 + k_2)$ and $K_2 = (k_{-1} + k_{-2})$ are designated as the total forward and backward rate constants. The pseudo first order rate constants k_1 and k_2 are given by $k_1 = k_1'[S]$ and $k_2 = k_2'[P]$.

The enzymatic activity can be manipulated by applying an external mechanical force. Here we have considered that a constant external mechanical force is applied on the single oligomeric enzyme at the chemiostatic condition. The external force helps to increase the dissociation of the ES complex because it decreases the activation barrier of breaking the ES complex. Following Bell's theory [42], we consider that if a constant external pulling force F is applied on the oligomeric enzyme, then the bonds between the identical active sites of the enzyme and the substrates experience the force, F cosθ as shown in Fig. 2. Here we consider that each identical bond experiences the same magnitude of force $Fcos\theta$, so the energy required to break a bond which is between one active site of the enzyme and a substrate is $FX_bcos\theta$, where X_b is the minimum elongation of a bond for dissociation. Here, a typical magnitude of X_b of 0.5Å is sufficient for bond rupture. The modified dissociation rate constants are given as $k_{-1,-2}^{(f)} = k_{-1,-2}e^f$ where $f = (FX_b\cos\theta/k_BT)$ [39,42].

The oligomeric enzyme kinetics reaction consists of four reaction channels or sub-reactions (see Fig. 1c). Due to the random occurrence of various reaction channels, the number of occupied sites becomes a fluctuating quantity. If at time t, n number of occupied sites are present in the system, i.e, the system is in the nth occupied state, then after a small time τ, the system goes to a new state, $(n + \nu_\mu)$ through any one of the four possible sub-reactions. Here ν_μ is designated as the stoichiometric coefficient of the μth reaction with rate constant k_μ. Now among n_T number of total active sites, if n number of sites form ES-complex at time t and $(n_T - n)$

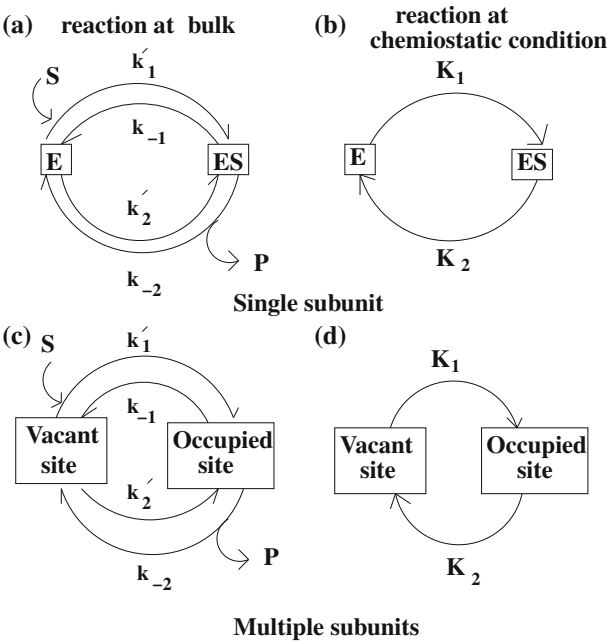

Fig. 1 Kinetic scheme of an enzyme having only one subunit is shown in bulk in (**a**) and in chemiostatic condition (**b**). Similar types of reaction schemes are represented for oligomeric enzyme having more than one subunit in (**c**, **d**), respectively. The rate constants $K_1 = (k_1 + k_2)$ and $K_2 = (k_{-1} + k_{-2})$ are designated as the total forward and backward rate constants. The pseudo first order rate constants k_1 and k_2 are given by $k_1 = k_1'[S]$ and $k_2 = k_2'[P]$

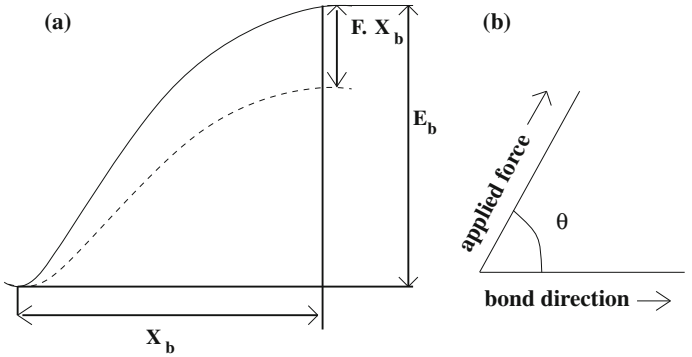

Fig. 2 **a** The *plot* depicts the activation energy, E_b as a function of the extension of bond along which the bond is ruptured. Here F is the externally applied mechanical force and X_b is the minimum elongation of the bond for dissociation. The force reduces the activation energy for the ES-complex dissociation and for large enough force, the dissociation becomes almost activationless. **b** The direction of the externally applied mechanical force makes an angle θ with the ES bond direction, so each bond between an active site of the enzyme and a substrate experience the force $F\cos\theta$

number of sites remain vacant, then the stochastic master equation can be written as

$$\frac{dP(n,t)}{dt} = \sum_{\mu=\pm1}^{\pm2} [w_\mu(n-\nu_\mu|n)P(n-\nu_\mu, t) - w_{-\mu}(n|n-\nu_\mu)P(n, t)] \tag{1}$$

where $\nu_\mu = 1$ with $\mu > 0$ and $-\nu_\mu = 1$ with $\mu < 0$; P(n, t) is the probability of having n number of occupied states at time t. The transition probabilities are defined as follows,

$$w_\mu(n-\nu_\mu|n) = k_\mu(n_T - (n-\nu_\mu)), \mu > 0$$

and

$$w_\mu(n-\nu_\mu|n) = k_\mu(n-\nu_\mu), \mu < 0. \tag{2}$$

Then Eq. (1) can be rewritten as

$$\begin{aligned}\frac{dP(n,t)}{dt} &= K_1(n_T - n + 1)P(n-1, t) + K_2(n+1)P(n+1, t) \\ &\quad -K_1(n_T - n)P(n, t) - K_2 nP(n, t).\end{aligned} \tag{3}$$

Solving the master equation by the standard approach of generating function method [39,43,44], we get the probability distribution function as

$$P(n,t) = \frac{n_T!}{n!(n_T - n)!} X^n Y^{n_T - n} \tag{4}$$

where $X = \frac{K_1(1-\exp(-(K_1+K_2)t))}{K_1+K_2}$, $Y = \frac{K_2+K_1\exp(-(K_1+K_2)t)}{K_1+K_2}$, assuming that initially all the active sites are unoccupied. With this initial condition, the time-dependent average number of occupied sites is given by $\langle n\rangle(t) = n_T X$ and the average number of vacant sites is $\langle n_T - n\rangle(t) = n_T Y$.

2.2 Entropy production rates from the master equation

The system entropy is defined in terms of the Shannon entropy as,

$$S_{sys}(t) = -k_B \sum_n P(n, t)\ln P(n, t). \tag{5}$$

We set the Boltzmann constant, $k_B = 1$. Using the above master equation, we get the system entropy production rate [40,45–47] as

$$\dot{S}_{sys}(t) = \frac{1}{2}\sum_{n,\mu}[w_\mu(n-\nu_\mu|n)P(n-\nu_\mu,t) - w_{-\mu}(n|n-\nu_\mu)P(n,t)] \times \ln\frac{P(n-\nu_\mu,t)}{P(n,t)}. \tag{6}$$

We have assumed ideal reservoir (surroundings) with no inherent ep except through the boundaries of the system. The system entropy production rate can be split as [46]

$$\dot{S}_{sys}(t) = \dot{S}_{tot}(t) - \dot{S}_m(t). \tag{7}$$

Here the first term in the r.h.s. of Eq. (7) gives the total entropy production rate and the second term denotes the medium entropy production rate due to the entropy flux into the surroundings. Therefore the total and medium entropy production rates are defined as

$$\dot{S}_{tot}(t) = \frac{1}{2}\sum_{n,\mu}[w_\mu(n-\nu_\mu|n)P(n-\nu_\mu,t) - w_{-\mu}(n|n-\nu_\mu)P(n,t)] \times \ln\frac{w_\mu(n-\nu_\mu|n)P(n-\nu_\mu,t)}{w_{-\mu}(n|n-\nu_\mu)P(n,t)} \tag{8}$$

and

$$\dot{S}_m(t) = \frac{1}{2}\sum_{n,\mu}[w_\mu(n-\nu_\mu|n)P(n-\nu_\mu,t) - w_{-\mu}(n|n-\nu_\mu)P(n,t)] \times \ln\frac{w_\mu(n-\nu_\mu|n)}{w_{-\mu}(n|n-\nu_\mu)}. \tag{9}$$

Using the expressions of the corresponding transition probabilities from Eq. (2) and the time dependent solution of the master equation, we finally obtain,

$$\dot{S}_{tot}(t) = \langle n(t)\rangle\left[k_{-1}\ln\left(\frac{k_{-1}X}{k_1Y}\right) + k_{-2}\ln\left(\frac{k_{-2}X}{k_2Y}\right)\right] - \langle n_T - n(t)\rangle\left[k_1\ln\left(\frac{k_{-1}X}{k_1Y}\right) + k_2\ln\left(\frac{k_{-2}X}{k_2Y}\right)\right]. \tag{10}$$

Now at the NESS, we use the condition of equality of forward and backward cycle flux instead of detailed balance condition [48]. Therefore, from Eq. (1), we obtain

$$w_1(n-1|n)P(n-1) - w_{-1}(n|n-1)P(n) = w_{-2}(n|n-1)P(n) - w_2(n-1|n)P(n-1). \tag{11}$$

By using Eq. (11) in Eq. (8), we obtain the total entropy production rate at the steady state as

$$\dot{S}_{tot}^{(ss)} = \sum_{n} \left[w_1(n-1|n)P(n-1) - w_{-1}(n|n-1)P(n) \right] \times \ln \left(\frac{w_1(n-1|n)P(n-1) \times w_{-2}(n|n-1)P(n)}{w_{-1}(n|n-1)P(n) \times w_2(n-1|n)P(n\text{-}1)} \right). \tag{12}$$

After putting the values of the transition probabilities, $\langle n \rangle$ and $\langle (n_T - n) \rangle$ at the steady state we obtain

$$\dot{S}_{tot}^{(ss)} = n_T \ln \left(\frac{k_{-1}k_2}{k_1 k_{-2}} \right) \left[\left(\frac{k_2 k_{-1} - k_1 k_{-2}}{k_1 + k_{-1} + k_2 + k_{-2}} \right) \right]. \tag{13}$$

At $\left(\frac{k_{-1}k_2}{k_1 k_{-2}} \right) = 1$, $\dot{S}_{tot}^{(ss)}$ becomes zero and the steady state corresponds to the detailed balance condition that holds in equilibrium. However, we are in general interested in the entropy production in the nonequilibrium steady state where $\left(\frac{k_{-1}k_2}{k_1 k_{-2}} \right) \neq 1$. Integrating $\dot{S}_{tot}$ between the time interval $t_0 = 0$ to t, we get the total entropy production, ΔS_{tot}. As we have considered that initially (time $t_0 = 0$) all the sub-units are vacant, i.e, n = 0 with P(n, 0) = 1, therefore, from Eq. 5, $S_{sys} = 0$ in the beginning.

3 Single trajectory analysis of entropy production and fluctuation theorem

In the previous section, the calculated total entropy production from the master equation is actually an average property. However, for a small system the fluctuation is as important as the average and from this to get an idea about the distribution we have calculated the total entropy production of an ensemble of trajectories. For a single trajectory, the system can be quantified in terms of the time series of the number of occupied sites of the oligomeric enzyme which is a fluctuating quantity due to the random occurrence of the reaction events within a short time interval. The time series of the number of occupied sites is calculated by using the Gillespie stochastic simulation approach [50,51].The simulated single trajectory of forward and backward path is used to calculate the total entropy production which varies from trajectory to trajectory as it is a fluctuating quantity.

Let us consider a stochastic trajectory of the number of occupied sites, n(t) which starts at n_0 and jumping at times t_j from n_{j-1} to n_j ending up at n_l with $t = t_l$,

$$n(t) \equiv (n_0, t_0) \xrightarrow{\nu_\mu^1} (n_1, t_1) \xrightarrow{\nu_\mu^2} \cdots \rightarrow (n_{j-1}, t_{j-1}) \xrightarrow{\nu_\mu^j} (n_j, t_j) \rightarrow \cdots \rightarrow (n_{l-1}, t_{l-1}) \xrightarrow{\nu_\mu^1} (n_l, t_l). \tag{14}$$

Here $n_j = n_{j-1} + \nu_\mu^j$ and $t_j = t_{j-1} + \tau_j$ where τ_j is the time interval between two successive jumps and j is the population state at time t. During the jump from the $(n_j - 1)$

state to the n_j state, any one of the four sub-reactions will occur and the time interval τ_j between the two jumps is a random variable following the exponential distribution

$$p(\tau_j) = a \quad \exp(-a\tau_j) \tag{15}$$

with $a = \sum_{\mu=\pm1}^{\pm2} w(n_j - 1;\, \nu_\mu^j)$ and $w(n_{j-1};\, \nu_\mu^j)$ denotes the transition probability from the state $(n_j - 1)$ to the n_j state through a reaction channel μ with the stoichiometric coefficient ν_μ^j along a single trajectory.

Now a time reversed trajectory can be defined as,

$$\begin{aligned} n^R(t) \equiv (n_l, t_l) &\overset{-\nu_\mu^l}{\rightarrow} (n_{l-1}, t_{l-1}) \overset{-\nu_\mu^{l-1}}{\rightarrow} \cdots \rightarrow (n_j, t_j) \\ &\overset{-\nu_\mu^j}{\rightarrow} (n_{j-1}, t_{j-1}) \cdots \rightarrow (n_1, t_1) \overset{-\nu_\mu^1}{\rightarrow} (n_0, t_0). \end{aligned} \tag{16}$$

This time reversed trajectory is generated due to the occurrence of a reaction channel whose state changing vector $-\nu_\mu^j$ is exactly opposite to the state changing vector ν_μ^j of the forward reaction channel.

The entropy production along a single stochastic trajectory can be defined as [28]

$$s(t) = -\ln P(n,\, t) \tag{17}$$

where $P(n, t)$ is the solution of the stochastic master equation for a given initial condition, $P(n_0, t_0)$, taken along the specific trajectory $n(t)$. Note that, the single trajectory entropy is denoted by s whereas the average entropy production, whether being an ensemble average obtained from the master equation or averaged over many trajectories generated in the simulation, is denoted by S. Now the time dependent total entropy production, Δs_{tot} can be split into a system part, Δs_{sys} and a medium contribution, Δs_m. Hence the change in total entropy along a trajectory can be written as [28,49,52]

$$\Delta s_{tot} = \Delta s_m + \Delta s_{sys} \tag{18}$$

where

$$\Delta s_{sys} = \ln \frac{P(n_0, t_0)}{P(n, t)} \tag{19}$$

and

$$\Delta s_m = \sum_j \ln \frac{w\left(n_{j-1};\, \nu_\mu^j\right)}{w\left(n_j;\, -\nu_\mu^j\right)}. \tag{20}$$

The ratio of probabilities of the forward trajectory path, $p(n(t)|n(t_0))$ and that of the backward trajectory path, $p(n^R(t)|n_l)$ of the reaction system is given by the quantity

$e^{\Delta s_{tot}}$, obtained by applying the stochastic simulation approach. For different trajectories we get different total entropy production values and among them some values may be negative, but the average total entropy production value must be positive. As the total entropy production values differ from trajectory to trajectory, so we get a distribution, $p(\Delta s_{tot})$. When the system reaches a steady state, the detailed fluctuation theorem is satisfied as

$$\frac{p(\Delta s_{tot})}{p(-\Delta s_{tot})} = e^{\Delta s_{tot}}. \tag{21}$$

Here we have studied the probability distribution function of entropy production in terms of the mean and variance of the distribution in the transient and steady state regime. We have numerically investigated how the negative values of total entropy appears in a single trajectory due to the applied force and the total number of active sites of the oligomeric enzyme or the system-size of the problem.

4 Numerical result and discussion

In this section we have calculated the entropy production, the average number of substrate binding and the net velocity of the reaction in the dynamic regime and non-equilibrium steady state for different applied forces. To obtain the medium entropy production as well as the distribution of the total entropy production we have constructed the time series of the number of occupied sites on the basis of single trajectory concept and it is adapted with the Gillespie's stochastic simulation approach.We have also studied the variation of mean, variance and the relative variance of the distribution with function of force at NESS. The studies at NESS give an important correspondence between the total entropy production rate and the net velocity of the reaction. To calculate the average substrate binding, $\langle n \rangle(t)$, the net velocity of the reaction and the various entropy production rates, we have taken the rate parameters as $k_1 = 15$, $k_{-1} = 7$, $k_{-2} = 2$ and $k_2 = 1$, all in s^{-1}, for both analytical and numerical studies. The total number of subunits of the single oligomeric enzyme is taken as $n_T = 20$.

Here we have determined the system and the medium entropy productions, for a single trajectory using the Gillespie's stochastic simulation approach. The corresponding macroscopic (ensemble average) quantities are then calculated from the averaging over the trajectories (2×10^5 in number) obtained from the simulation. We have plotted ΔS_m, ΔS_{sys} and ΔS_{tot} in Fig. 3 as a function of time determined at different forces. The time evolution of average number of occupied sites, $\langle n \rangle(t)$ at different forces are also shown. ΔS_{tot} and $\langle n \rangle$ are determined from the simulation as well as from the analytical expression to provide a check of the simulation results. Now the determination of ΔS_{sys} from Eq. (19) uses the analytical solution of the master equation, $P(n, t)$ at various points of time.The plot of ΔS_m, as shown in Fig. 3a, increases with time, initially at a faster rate for lower value of force but eventually the rate becomes higher for the larger force. ΔS_{tot}, obtained from simulation as well as from Eq. (10), shows similar behavior as a function of the force parameter regarding the values at short and long times as shown in Fig. 3c. In Fig. 3b, we have plotted the variation of ΔS_{sys}. After a small time, ΔS_{sys} reaches a steady value as the reaction system reaches the NESS.

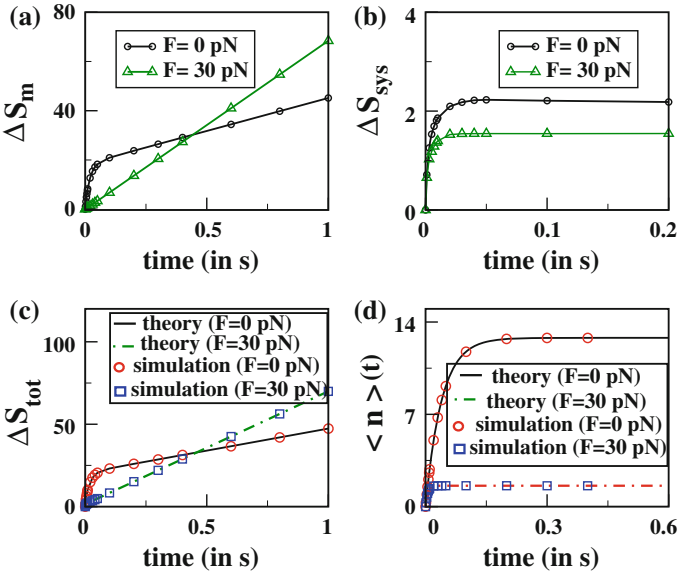

Fig. 3 Plot of **a** ΔS_m, **b** ΔS_{sys}, **c** ΔS_{tot} and **d** $\langle n \rangle (t)$ versus time for force parameters, F = 0 and F = 30 pN. The rate parameters are the same as given in Fig. 1 caption

With increase in force, it reaches the steady value earlier and the magnitude of ΔS_{sys} decreases with increase in force. As the magnitude of ΔS_{sys} is small compared to the value of ΔS_m, hence the nature of the curve of ΔS_m versus time follows the ΔS_{tot} versus time plot and at the NESS they grow linear in time. At $t \to \infty$, $\Delta S_m \to \Delta S_{tot}$ which is very useful when ΔS_{sys} is not known, for example, when no rate equation is available although the detailed steps of the reaction may be known. Finally, one can see from Fig. 3d that $\langle n \rangle (t)$ decreases significantly with the application of force as the force increases the dissociation rate of the ES-complex. Its variation with time and the force is similar to that of ΔS_{sys}. It is evident from the figures that the transient and NESS characteristics of the reaction are exactly followed by the system entropy production. However, the medium entropy production which is mainly concerned with the flow through the boundaries of the system, actually takes care of the total entropy production at NESS when the system property saturates; one can identify the boundary effect of the system by its size and physical or chemical nature of interactions between the system and surroundings in terms of the medium entropy.

The entropy production, Δs_{tot} along a single trajectory is a fluctuating quantity; it has a distribution, $p(\Delta s_{tot})$, which is shown in Fig. 4a, b at different time intervals for force values $F = 0$ and $F = 30$ pN, respectively with $n_T = 20$. At short times, the distribution is non-Gaussian in nature but gradually tends to a Gaussian distribution which is obtained due to the chemiostatic condition of the open system at NESS. It is evident from the figure that initially there is a non-zero probability of observing negative values of Δs_{tot} for a particular trajectory with $F = 30$ pN whereas for $F = 0$ pN, such probability is zero for the rate parameters considered here. We have found that with rise in the magnitude of the force, the probability of observing negative values

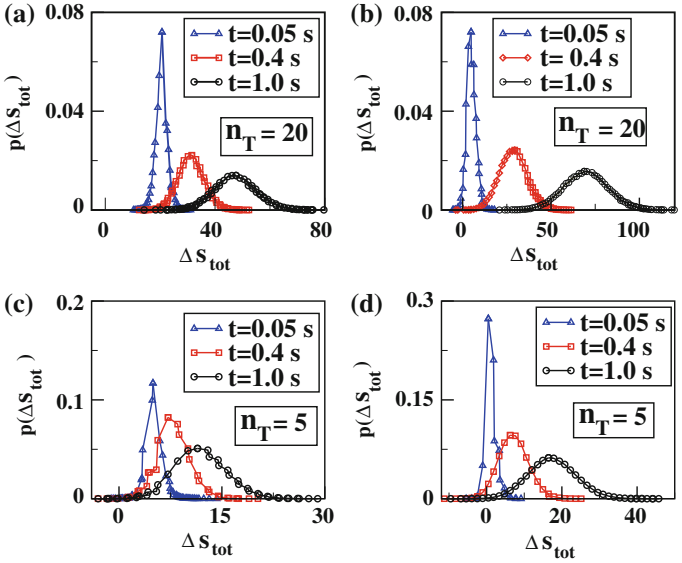

Fig. 4 The distribution of the total entropy production over trajectories, $p(\Delta s_{tot})$ versus Δs_{tot} is plotted for different times in (**a**, **b**) with force, F = 0 and F = 30 pN, respectively with $n_T = 20$. The corresponding plots for $n_T = 5$ are shown in (**c**, **d**)

of Δs_{tot} first increases but then saturates (not shown in figures). Although the mean value can be obtained from the master equation, the broadening of the distribution due to the increase in external force can only be realized through the trajectory based method.

By comparing the distributions in Fig. 4a, b at different times, one can see that the overall distribution quickly shifts to the positive zone reaching larger positive values with increased force. These simulation results provide the microscopic basis for the macroscopic result of the initially lower ΔS_{tot} for higher forces and explains how ΔS_{tot} becomes higher for the same higher forces at some later time. The larger probability for negative Δs_{tot} values under the $p(\Delta s_{tot})$ distribution curve at higher forces brings the average value, ΔS_{tot} down at short times. Now similar results are given in Fig. 4c, d for $n_T = 5$. By comparing these plots with those for $n_T = 20$ reveals that for lower system size, there is a larger probability to realize entropy consuming trajectories as here the distribution, $p(\Delta s_{tot})$ can initially span larger negative regions, particularly at higher forces. The total entropy production distribution for $n_T = 5$ is always shifted to the left compared to that for $n_T = 20$ and this gives the microscopic basis of the extensive nature of the entropy production.

With decrease in the system size the probability of obtaining the entropy consuming trajectories is increased. It is customary to have a finite region of the distribution, $p(\Delta s_{tot})$ with negative values of Δs_{tot} to explicitly show the detailed fluctuation theorem at steady state [25]. Initially, with increase in the value of rate parameter k_2 increases the probability of finding the entropy consuming trajectories. We have observed that in the ideal Michaelis–Menten type enzyme kinetics reaction where k_2

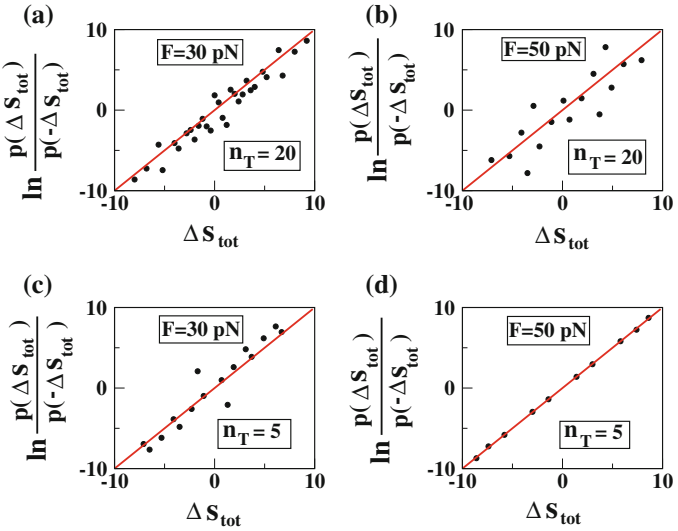

Fig. 5 $\ln\left(\frac{p(\Delta s_{tot})}{p(-\Delta s_{tot})}\right)$ versus Δs_{tot} is plotted in (**a**), **b** for $n_T = 20$ with force, F = 30 and F = 50 pN, respectively. Similar plots are drawn in **c**, **d** for $n_T = 5$ with same force parameters

value is very very small, probability of obtaining the entropy consuming trajectories is almost zero. It is also important to note that with increase in the values of force parameters, probability of entropy consuming trajectories is increased and that's why we have verified the fluctuation theorem at force F = 30 and F = 50 pN which is shown in Fig. 5. We have plotted, $\ln\frac{p(\Delta s_{tot})}{p(-\Delta s_{tot})}$ versus Δs_{tot} in the range $-10 < \Delta s_{tot} < 10$ for $n_T = 20$ in Fig. 5a, b at F = 30 and F = 50 pN, respectively and for $n_T = 5$ in Fig. 5c, d for the same force values. It is evident from the figure that the total entropy production of the reaction system satisfy the detailed fluctuation theorem at the steady state.

From the simulation data, we also analyze the variance and the mean of the total entropy production distribution, $p(\Delta s_{tot})$. The mean total entropy production is obviously equal to the results already obtained from the analytical approach. Now from Fig. 6a, we see that both the mean and the variance of $p(\Delta s_{tot})$, determined at the NESS, first increases but then saturates with the applied force. The saturation at large force is associated with almost instantaneous dissociation of the ES-complex when the net rate of product formation reaches a limiting value with an activationless transition [39]. The relative variance of the distribution decreases with the external force at the NESS which is shown in Fig. 6b. It indicates that the higher force makes the system more deterministic. Due to the high dissociation rate, a ES-complex breaks readily immediately after formation. So the population of the occupied state mainly oscillates between 0 and 1 and the system behaves more deterministically.

We have also shown the time evolution of the variance in Fig. 6c at three different forces, $F = 0, F = 10$ and $F = 30$ pN. It is evident that except some transient behavior, the variance increases linearly with time as the system reaches and stays at the NESS. It amounts to the fact that the entropy production distribution obeys a driven diffusion

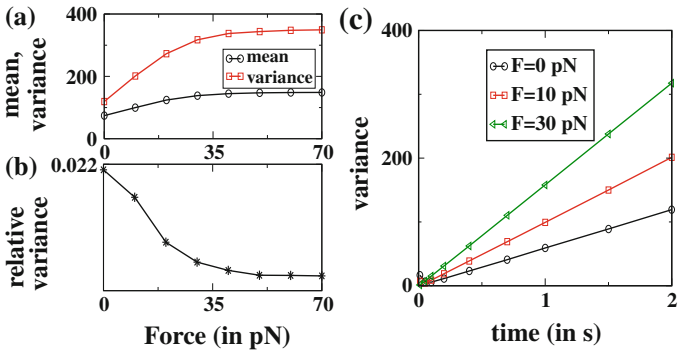

Fig. 6 **a** The mean and variance of the total entropy production distribution, $p(\Delta s_{tot})$ as a function of the external force determined at the NESS. **b** The relative variance is plotted against applied force at NESS. **c** The evolution of variance of $p(\Delta s_{tot})$ with time for force F = 0,10 and F = 30 pN

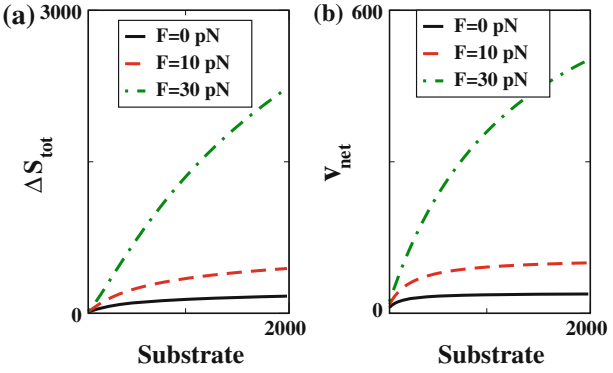

Fig. 7 **a** *Plot* of total entropy production versus substrate at NESS with force values F = 0, F = 10 and F = 30 pN. **b** The evolution of net velocity, v_{net} with substrate is plotted at NESS for same force values

process at the NESS with a time-independent diffusion coefficient which implies the variance of entropy production distribution increases linearly with time for a particular value of applied force. The diffusion coefficient increases with increase in force before going to saturation.The mean and variance of the Gaussian distribution of the total entropy production at NESS behaves almost in a similar fashion with the applied force.

We have also calculated the total entropy production rate at NESS as a function of the substrate population for different force values. The rate increases with substrate population in a hyperbolic fashion as is usually observed both in the bulk and single enzyme catalysis and the rise of force makes the entropy production rate larger. We have compared this entropy production rate variation with the corresponding variation of the net velocity of the reaction, v_{net} in Fig. 7a, b. It is evident that v_{net} rises with the substrate population and the applied force in a similar manner as that of the entropy production rate. From Figs. 3 and 7, it is evident that reaction characteristics follow

the ΔS_{sys} curve as a function of time whereas at the NESS, they follow the ΔS_{tot} curve as a function of the substrate population.

5 Conclusion

In this work, we have studied the entropy production rate for a single oligomeric enzyme kinetics under chemiostatic condition with an externally controllable mechanical force that affects the net rate of the product formation through the substrate binding. The progress of the reaction is described through a chemical master equation. To get a microscopic view, we have also used the single stochastic trajectory approach of calculating the entropy production with Gillespie's stochastic simulation algorithm.

We have thoroughly analyzed the effect of the external force on the reaction characteristics like the net velocity and the eps. At the nonequilibrium steady state the rate of the reaction and entropy production rate follow the similar hyperbolic trend with substrate population for various forces. We have found that the time-variation of the system entropy production is qualitatively similar to that of the average substrate binding at different forces. From the single trajectory stochastic simulation data, we have analyzed the evolution of the distribution of the total entropy production as a function of time and the applied force. We have found that with increase in force, an increased probability of entropy consuming trajectories can be obtained which becomes more prominent for lower system-size. All these results are constrained by the detailed fluctuation theorem which maintains the corresponding entropy production distribution.

The mean value of the distribution of entropy production obtained from the ensemble of single trajectories corresponds to the results obtained from the master equation. However, it indicates a new effect of the external force on the distribution of entropy production which is akin to power broadening of the distribution. The variance of entropy production increases linearly with time for a particular value of applied force indicating that the entropy production distribution obeys a a driven diffusion equation at the NESS. Both the mean and the variance of the Gaussian distribution of entropy production, determined at a particular instant of NESS, first increases but then saturates with the rise in applied force. This is due to the instantaneous dissociation of the ES-complex when the net rate of product formation reaches a limiting value with a 'barrierless' transition. In mechanochemistry, an external force being another controllable thermodynamic variable over the traditional variables of temperature and pressure, which can be used to find out the variance of the entropy production in small systems where the fluctuation is as important as the mean value.

Acknowledgments K.B. acknowledges the Council of Scientific and Industrial Research (C.S.I.R.) for the partial financial support as a Senior Research Fellow.

References

1. D. Collin, F. Ritort, C. Jarzynski, S.B. Smith, I. Tinoco Jr., C. Bustamante, Nature **437**, 231 (2005)
2. C. Jarzynski, Nat. Phys. **7**, 591 (2011)
3. J. Liphardt, S. Dumont, S.B. Smith, I. Tinoco Jr., C. Bustamante, Science **296**, 1832 (2002)
4. H. Wang, G. Oster, Nature **396**, 279 (1998)

5. D.M. Carberry, M.A.B. Baker, G.M. Wang, E.M. Sevick, D.J. Evans, J. Opt. A Pure Appl. Opt. **9**, S204 (2007)
6. G. Hummer, A. Szabo, Proc. Natl. Acad. Sci. USA **98**, 3658 (2001)
7. F. Ritort, C. Bustamante, I. Tinoco Jr., Proc. Natl. Acad. Sci. USA **99**, 13544 (2002)
8. C. Bustamante, J. Liphardt, F. Ritort, Phys. Today **58**, 43 (2005)
9. A. Mossa, S. De Lorenzo, J.M. Huguet, F. Ritort, J. Chem. Phys. **130**, 234116 (2009)
10. M. Manosas, A. Mossa, N. Forns, J.M. Huguet, F. Ritort, J. Stat. Mech.: Theor. and Expt. **09**, P02061 (2009)
11. F. Ritort, Adv. Chem. Phys. **137**, 31 (2008)
12. I. Tinoco Jr., C. Bustamante, Biophys. Chem. **101**, 513 (2002)
13. C. Bustamante, Y.R. Chemla, N.R. Forde, D. Izhaky, Annu. Rev. Biochem. **73**, 705 (2004)
14. C. Jarzynski, Phys. Rev. Lett. **78**, 2690 (1997)
15. C. Jarzynski, Phys. Rev. E **56**, 5018 (1997)
16. G.E. Crooks, J. Stat. Phys. **90**, 1481 (1998)
17. G.E. Crooks, Phys. Rev. E **60**, 2721 (1999)
18. U. Seifert, Phys. Rev. Lett. **95**, 040602 (2005)
19. T. Hatano, S.I. Sasa, Phys. Rev. Lett. **86**, 3463 (2001)
20. M. Esposito, C. Vanden Broeck, Phys. Rev. Lett. **104**, 090601 (2010)
21. D.J. Evans, E.G.D. Cohen, G.P. Morriss, Phys. Rev. Lett. **71**, 2401 (1993)
22. G. Gallavotti, E.G.D. Cohen, Phys. Rev. Lett. **74**, 2694 (1995)
23. G. Gallavotti, Phys. Rev. Lett. **77**, 4334 (1996)
24. J.L. Lebowitz, H. Spohn, J. Stat. Phys. **95**, 333 (1999)
25. S. Lahiri, A.M. Jayannavar, Eur. Phys. J. **B69**, 87 (2009)
26. E.M. Sevick, R. Prabhakar, S.R. Williams, D.J. Searles, Annu. Rev. Phys. Chem. **59**, 603 (2008)
27. T. Schmiedl, U. Seifert, J. Chem. Phys. **126**, 044101 (2007)
28. V. Blickle, T. Speck, L. Helden, U. Seifert, C. Bechinger, Phys. Rev. Lett. **96**, 070603 (2006)
29. C. Tietz, S. Schuler, T. Speck, U. Seifert, J. Wrachtrup, Phys. Rev. Lett. **97**, 050602 (2006)
30. T. Schmiedl, T. Speck, U. Seifert, J. Stat. Phys. **128**, 77 (2007)
31. U. Seifert, Europhys. Lett. **70**(1), 36 (2005)
32. A.P. Wiita, S.R.K. Ainavarapu, H.H. Huang, J.M. Fernandez, Proc. Natl. Acad. Sci. USA **103**, 7222 (2006)
33. A.P. Wiita, R. Perez-Jimenez, K.A. Walther, F. Grater, B.J. Berne, A. Holmgren, J.M. Sanchez-Ruiz, J.M. Fernandez, Nature **450**, 124 (2007)
34. H. Gumpp, E.M. Puchner, J.L. Zimmermann, U. Gerland, H.E. Gaub, K. Blank, Nano Lett. **9**, 3290 (2009)
35. A.S. Adhikari, J. Chai, A.R. Dunn, J. Am. Chem. Soc. **133**, 1686 (2011)
36. H.P. Lu, L. Xun, X.S. Xie, Science **282**, 1877 (1998)
37. S.C. Kou, B.J. Cherayil, W. Min, B.P. English, X.S. Xie, J. Phys. Chem. B **109**, 19068 (2005)
38. S. Yang, J. Cao, J. Chem. Phys. **117**, 10996 (2002)
39. B. Das, G. Gangopadhyay, J. Chem. Phys. **132**, 135102 (2010)
40. D. Andrieux, P. Gaspard, J. Chem. Phys. **121**, 6167 (2004)
41. I. Migneault, C. Dartiguenave, M.J. Bertrand, K.C. Waldron, BioTechniques **37**, 790 (2004)
42. G. Bell, Science **200**, 618 (1978)
43. C.W. Gardiner, *Handbook of Stochastic Methods for Physics, Chemistry and the Natural Sciences*, 2nd edn. (Springer, New York, 1985)
44. N.G. Vankampen, *Stochastic Processes in Physics and Chemistry Amsterdam* (Elsevier, The Netherlands, 1992)
45. P. Gaspard, J. Chem. Phys. **120**, 8898 (2004)
46. L. Jiu-li, C. Vanden Broeck, G. Nicolis, Z. Phys. B **56**, 165 (1984)
47. G. Nicolis, I. Prigogine, *Self-Organization in Nonequilibrium Systems* (Willey, New York, 1977)
48. M. Vellela, H. Qian, J.R. Soc. Interface **6**, 925 (2009)
49. T.J. Xiao, Z. Hou, H. Xin, J. Chem. Phys. **129**, 114506 (2008)
50. D.T. Gillespie, J. Comput. Phys. **22**, 403 (1976)
51. D.T. Gillespie, J. Phys. Chem. **81**, 2340 (1977)
52. J. Luo, N. Zhao, B. Hu, Phys. Chem. Chem. Phys. **4**, 4149 (2002)